Dynamics of Klebsiella pneumoniae OmpA transmembrane domain: The four extracellular loops display restricted motion behavior in micelles and in lipid bilayers

Iordan Iordanov, Marie Renault, Valérie Réat, Patrick Bosshart, Andreas Engel, Olivier Saurel, Alain Milon

Biochimica et Biophysica Acta 1818 (2012) 2344–2353

Contents lists available at SciVerse ScienceDirect

Biochimica et Biophysica Acta

journal homepage: www.elsevier.com/locate/bbamem

Dynamics of *Klebsiella pneumoniae* OmpA transmembrane domain: The four extracellular loops display restricted motion behavior in micelles and in lipid bilayers

Iordan Iordanov [a,b], Marie Renault [c], Valérie Réat [a,b], Patrick D. Bosshart [d], Andreas Engel [e], Olivier Saurel [a,b], Alain Milon [a,b,*]

[a] *Institute of Pharmacology and Structural Biology, Université de Toulouse, UPS, 205 route de Narbonne, 31077 Toulouse, France*
[b] *IPBS, UMR 5089, CNRS, 205 route de Narbonne, BP 64182, 31077 Toulouse, France*
[c] *UPCAM iSm2 service 512, Campus Scientifique de St Jérôme, 13397 Marseille cedex 20, France*
[d] *Department of Biosystems Science and Engineering, ETH Zurich, CH-4058 Basel, Switzerland*
[e] *Department of Pharmacology, Case Western Reserve University, Cleveland, OH 44106, USA*

ARTICLE INFO

Article history:
Received 21 February 2012
Received in revised form 2 May 2012
Accepted 3 May 2012
Available online 9 May 2012

Keywords:
Outer membrane protein A
Protein reconstitution
Protein dynamics
Spin–lattice relaxation
Solid-state NMR
Electron microscopy

ABSTRACT

The transmembrane domain of *Klebsiella pneumoniae* OmpA (KpOmpA) possesses four long extracellular loops that exhibit substantial sequence variability throughout OmpA homologs in *Enterobacteria*, in comparison with the highly conserved membrane-embedded β-barrel core. These loops are responsible for the immunological properties of the protein, including cellular and humoral recognition. In addition to key features revealed by structural elucidation of the KpOmpA transmembrane domain in detergent micelles, studies of protein dynamics provide insight into its function and/or mechanism of action. We have investigated the dynamics of KpOmpA in a lipid bilayer, using magic angle spinning solid-state NMR. The dynamics of the β-barrel and loop regions were probed by the spin–lattice relaxation times of the C^{α} and C^{β} atoms of the serine and threonine residues, and by cross-polarization dynamics. The β-barrel core of the protein is rigid; the C-terminal halves of two of the four extracellular loops (L1 and L3), which are particularly long in KpOmpA, are highly mobile. The other two loops (L2 and L4), which are very similar to their homologs in *Escherichia coli* OmpA, and the N-terminal halves of L1 and L3 exhibit more restricted motions. We suggest a correlation between the sequence variability and the dynamics of certain loop regions, which accounts for their respective contributions to the structural and immunological properties of the protein.

1. Introduction

Membrane proteins represent approximately one-third of all proteins in living organisms [1], are involved in many key physiological processes, and are favored targets for therapeutic drug development [2]. Detailed investigation of membrane protein structure, dynamics and molecular interactions in functional environments is, therefore, a major challenge for structural biology.

Recent advances in NMR spectroscopy have provided unique opportunities to probe the structure of integral membrane proteins at atomic resolution, as well as their associated molecular motions over a large time scale, under different conditions [3,4]. A combination of refined isotope-labeling schemes and multidimensional transverse-relaxation optimized spectroscopy (TROSY)-based solution-state NMR experiments can be used to determine the entire 3D molecular structures of small to medium-size β-barrel and α-helical integral membrane proteins in membrane mimetic environments, provided that molecular entities tumble rapidly [5,6]. Solid-state NMR (ssNMR) spectroscopy offers a complementary spectroscopic tool to monitor the molecular structure and dynamics of larger integral membrane proteins at atomic resolution and in complex settings, such as membrane bilayers [7,8].

We have previously determined the 3D structure the 210-residue TM domain of the outer membrane protein A from *Klebsiella pneumoniae* (KpOmpA) in DHPC detergent micelles [9]. *K. pneumoniae* is a Gram-negative bacterium that is responsible for respiratory tract and urinary infections. KpOmpA belongs to the OmpA family of proteins that is well conserved among *Enterobacteria* and has diverse roles in bacterial cellular processes [10–12]. For example, OmpA can function as an adhesin and invasin, participates in biofilm formation, acts as both an

Abbreviations: KpOmpA, *Klebsiella pneumoniae* outer membrane protein A; TM, transmembrane; LPR, lipid to protein ratio; CMC, critical micellar concentration; PLE, *E. coli* Polar Lipid Extract; OG, *n*-octyl-β-D-glucopyranoside; DHPC, 1,2-dihexanoyl-*sn*-glycero-3-phosphocholine; DOPC, 1,2-dioleoyl-sn-glycero-3-phosphocholine; DMPC, 1,2-dimyristoyl-sn-glycero-3-phosphocholine; ssNMR, solid state Nuclear Magnetic Resonance; PDSD, proton-driven spin diffusion; CP, cross-polarization

* Corresponding author at: Institute of Pharmacology and Structural Biology, IPBS, UMR 5089, Université de Toulouse, UPS and CNRS, 205 route de Narbonne, BP 64182, 31077 Toulouse Cedex 04, France. Tel.: +33 5 61 17 54 23; fax: +33 5 61 17 59 94.
E-mail addresses: iordan.iordanov@ipbs.fr (I. Iordanov), marie31.renault@gmail.com (M. Renault), valerie.reat@ipbs.fr (V. Réat), patrick.bosshart@bsse.ethz.ch (P.D. Bosshart), andreas.engel@case.edu (A. Engel), olivier.saurel@ipbs.fr (O. Saurel), alain.milon@ipbs.fr (A. Milon).

0005-2736/$ – see front matter © 2012 Elsevier B.V. All rights reserved.
doi:10.1016/j.bbamem.2012.05.004

immune target and evasin, and serves as a receptor for several bacteriophages [13]. Pore-forming activity of KpOmpA has been reported [14] and subsequently debated [13,15]. Although sequence conservation within the OmpA family is particularly high in the TM domain (~80%), the extracellular loops exhibit larger variability in terms of length and amino-acid sequence. Interestingly, the extracellular loops of KpOmpA appear to play important roles in the immunological properties of the protein, such as cellular recognition mediated by the scavenger receptors LOX-1 and SREC-I, and humoral recognition mediated by the long pentraxin PTX3 [11,16]. When solubilized in DHPC micelles, the structure of the TM domain of KpOmpA (Met3-Glu207) consists in an antiparallel 8-stranded β-barrel with four extracellular loops of different lengths and three short periplasmic turns that closely mirror available 3D structures of *Escherichia coli* OmpA TM domains [17–20]. We reported that the KpOmpA TM domain in DHPC micelles exhibits a mobility gradient, with mobility increasing from the β-barrel core toward the extracellular loops [9]. Although the center of the β-barrel is highly rigid, the protein segments that surround the two aromatic girdles at the interface exhibit sizable motions on the millisecond time scale. Finally, the extracellular loops are disordered and characterized by nanosecond time-scale motions of different amplitudes.

Key to further characterization of KpOmpA is the investigation of its structure and dynamics at atomic resolution in native-like environments, such as lipid bilayers, where lateral pressure [21], membrane curvature [22], lateral organization, domain formation [23] and protein oligomerization [24,25] occur and may play important roles in the protein structure, dynamic and function. In order to achieve this aim, we reconstituted the uniformly [^{13}C, ^{15}N]-labeled KpOmpA TM domain in lipid bilayers from a well-folded and soluble form in detergent micelles, and have investigated the folding and dynamics of the protein using ssNMR spectroscopy under magic angle spinning (MAS) conditions. First, the reconstitution of KpOmpA in lipid bilayers was optimized. Successful reconstitutions with a lipid-to-protein ratio (LPR) equal to or below 0.5 (w/w) were analyzed by electron microscopy (EM) to monitor sample homogeneity and the presence of protein patches. Then, KpOmpA-containing proteoliposomes were analyzed by ssNMR spectroscopy to probe the folding and local dynamics of the protein. Using 1- and 2D ssNMR experiments employing either scalar- or dipolar-based magnetization transfer steps associated with ^{13}C spin–lattice relaxation measurements and cross-polarization dynamics, we assessed the dynamics of the KpOmpA membrane domain in bilayers composed of *E. coli* polar lipid extracts. A new and refined picture of the loops dynamics emerges from the comparison of ssNMR data in lipid bilayers and heteronuclear NOE data previously obtained in a micellar environment [9].

2. Materials and methods

2.1. Expression, purification and detergent exchange

The cloning, expression and purification of *K. pneumoniae* outer membrane protein A (KpOmpA) TM domain were performed as described previously [9]. For the small-scale reconstitution trials and sucrose gradient centrifugation, the unlabeled protein was purified from *E. coli* BL21 (DE3) culture grown in Terrific Broth (Invitrogen) medium. For NMR experiments, the bacteria were grown in M9 minimal medium supplemented with 2 g/l $^{15}NH_4Cl$ and 2 g/l U-$^{13}C_6$ D-glucose (Cambridge Isotope Laboratories, Inc.) as the only nitrogen and carbon sources, respectively, producing uniformly [^{13}C, ^{15}N]-labeled KpOmpA TM domain.

For detergent exchange, purified KpOmpA/Zwittergent 3–14 complexes were incubated with nickel-chelating resin (Ni-NTA Superflow, QIAGEN) for 3 h at 4 °C under gentle mixing. The resin-bound protein was washed three times with 50 ml of 25 mM Tris/HCl (pH 8.5), 150 mM NaCl, 2% *n*-octyl-β-D-glucopyranoside (OG, Anatrace) and isolated by centrifugation (4000 *g*, 10 min, 4 °C). The KpOmpA/OG complexes were then eluted in one step with 25 mM Tris/HCl (pH 8.5), 150 mM NaCl, 2% OG and 400 mM imidazole. The concentration of the purified protein (either in 0.1% Zwittergent 3–14 or in 2% OG micelles) was determined spectrophotometrically by measuring absorbance at 280 nm and using the theoretical protein molar extinction coefficient of 50880 M^{-1} cm^{-1}. The successful refolding of the protein in both detergents was checked with SDS PAGE [26].

2.2. Reconstitution

Protein reconstitution was examined in three types of lipid: DOPC, DMPC and *E. coli* polar lipid extract (PLE) (all from Avanti Polar Lipids). Proteoliposomes containing the TM domain of KpOmpA were prepared using a detergent dilution method adapted from procedures described by Rigaud et al. [27]. Briefly, each lipid type was dissolved in chloroform, and dried under a stream of nitrogen gas and then in a vacuum chamber overnight. Mixed micelles were prepared by hydration of the lipid film with 25 mM Tris/HCl (pH 8.5), 150 mM NaCl and 2% OG with a final lipid concentration of 6 or 10 mg/ml. Purified and unlabeled monomeric KpOmpA TM domain (at a concentration of 1–3 mg/ml, depending on the different preparations) was added to the mixed micelles solution at the desired lipid-to-protein ratio (LPR) and incubated for 10 min at 4 °C. The solution of KpOmpA/OG/lipid ternary complexes was then dialyzed twice (12 h each) against 2 l of the desired detergent-free buffer at 37 °C to achieve the complete removal of detergent and imidazole and the formation of large unilamellar vesicles (LUVs). In order to screen a large panel of experimental conditions, the reconstitution trials were conducted in dialysis buttons of ~70 µl volume. The LPRs tested were between 0.1 and 1 (in 0.1 steps), 10 and 20 (w/w). The different dialysis buffers used in these small-scale reconstitution trials were: Buffer A (140 mM NaCl, 20 mM HEPES, pH 7.0), Buffer B (300 mM NaCl, 20 mM HEPES, pH 7.0), Buffer C (100 mM NaCl, 20 mM Tris, pH 8.5), Buffer D (140 mM NaCl, 20 mM Tris, pH 8.5) and Buffer E (300 mM NaCl, 20 mM Tris, pH 8.5). All buffers contained 0.01% NaN_3 to prevent the growth of contaminating bacteria.

2.3. NMR sample preparation

For solid-state NMR (ssNMR) experiments, 22 mg of purified, uniformly [^{13}C, ^{15}N]-labeled KpOmpA in 25 mM Tris buffer (pH 8.5) containing 150 mM NaCl and 2% OG was reconstituted in 11 mg of *E. coli* PLE as described above, resulting in an LPR of 0.5 (w/w), equal to a molar ratio of ~15 lipid molecules per protein molecule. The mixture was transferred to a dialysis tube with a 12–14 kDa cutoff (SpectraPor) and dialyzed twice against 2 l of 25 mM Tris/HCl (pH 8.5), 150 mM NaCl. Following the removal of detergent and imidazole, and the formation of LUVs during the first two dialysis steps, the dialysis buffers were exchanged every 12 h with a gradual decrease in the concentration of NaCl in 25-mM steps until the salt was completely removed. The size of the resulting proteoliposomes was verified by dynamic light scattering (DynaPro NanoStar, Wyatt Technology Corporation) and had a major population of particles that were ~1–3 µm in diameter (data not shown). The LUVs were collected by centrifugation (200 000 *g*, 90 min, 10 °C) and partially dehydrated under a stream of nitrogen gas until the total sample weight was reduced to ~50 mg. This value corresponded to approximately 33 mg of protein/lipid material with an LPR of 0.5 (w/w) and 17 mg water (30 w/v% of the entire sample). The proteoliposomes were then transferred to a 4-mm magic angle spinning (MAS) rotor by low-speed centrifugation (3000 *g*, 10 min, 10 °C) and subsequently analyzed by ssNMR spectroscopy.

2.4. Sucrose gradient centrifugation and colorimetric assays

Unlabeled KpOmpA-containing liposomes prepared in exactly the same way as the ssNMR sample (but not dehydrated under a stream of nitrogen gas) were collected (15 000 *g*, 20 min, 4 °C) and subjected to centrifugation at 4 °C in a 20–60% continuous sucrose gradient for

18 h at 100 000 *g* in SW41 rotor (Beckman) for an assessment of homogeneity and verification of the LPR. The isolated single band was subsequently analyzed for protein content by Lowry titration [28] and for lipid content by phosphoric acid titration [29].

2.5. Transmission electron microscopy

The reconstitution of KpOmpA into lipid bilayers was checked by transmission electron microscopy. For that purpose the sample was adsorbed to a carbon-coated copper grid, which was rendered hydrophilic by glow discharge at low pressure. The grids were then washed in nanopure water (resistivity > 18 MΩ·cm), stained with 2% (w/v) uranyl acetate, blotted and air-dried. Electron micrographs were recorded on a charge-coupled device (CCD) with a CM100 transmission electron microscope (FEI, Eindhoven, Netherlands) operated at 80 kV acceleration voltage.

2.6. NMR spectroscopy

ssNMR experiments were carried out on a Bruker AVANCE standard-bore NMR spectrometer (Bruker Biopsin) operating at a ^{1}H Larmor frequency of 700 MHz and equipped with a 4 mm-double resonance ^{1}H-{^{15}N–^{13}P} cross-polarization (CP)-MAS probe. The MAS frequency was set to 12 kHz and the sample temperature was regulated at 20 °C. The typical π/2 pulse length for ^{1}H was 3.1 μs. Unless otherwise indicated, the ^{1}H–^{13}C CP magnetization transfer step employed a linear ramp (50 to 100% field strength) on the ^{1}H channel. 1D CP-MAS spectra were obtained using a CP contact time of 400 μs and a ^{13}C radio frequency field of 60 kHz. High-power proton decoupling was obtained using TPPM [30] schemes and a decoupling field of 80 kHz. 2D ^{13}C–^{13}C proton-driven spin diffusion (PDSD) [31] experiments were performed using similar acquisition parameters and a PDSD mixing time of 40 ms. The ^{13}C spin–lattice relaxation measurements were achieved using 2D T_1-edited (^{13}C–^{13}C) PDSD correlation experiments (i.e., with a 90°–τ–90° element between the ^{1}H–^{13}C CP and t_1 evolution period). Spectra were obtained for nine spin–lattice relaxation times (0.02, 10, 100, 250, 500, 700, 1000, 2000 and 4000 ms), using 48 scans for each of the 364 t_1 increments. Characteristic C^{α}–C^{β} cross-peaks of Thr and Ser residues were integrated. Cross-peak integrals were plotted as a function of the T_1 relaxation delay (τ) and fitted using a mono-exponential decay function to determine T_1 relaxation time. The CP dynamics measurement relied on 13 2D ^{13}C–^{13}C PDSD correlation experiments using 76 scans for each 256 t_1 increments and employing CP contact times of 0.025, 0.05, 0.1, 0.15, 0.2, 0.3, 0.4, 0.5, 0.6, 1, 2, 4 and 8 s. Cross-peaks intensities of Thr and Ser C^{α}–C^{β} were plotted as a function of the CP contact time and fitted with the equation of the two-stage model to determine the T_{CP} and $T_{1\rho}$ values [32]. Uncertainty in values was determined from the standard errors of the fitting. 1D (^{1}H)–^{13}C refocused-INEPT (with $^{1}J_{CH}$ of 142 Hz) and ^{13}C direct excitation experiments employed π/2 pulse lengths of 3.1 μs (^{1}H) and 4 μs (^{13}C), corresponding to ^{1}H and ^{13}C RF fields of 80 and 62 kHz, respectively. Similarly to CP-based ssNMR experiments, proton decoupling was achieved using SPINAL64 schemes [33] and a decoupling field of 80 kHz. For ^{13}C direct and CP measurements, 2 K scans were acquired, and 12 K scans were acquired for the refocused-INEPT experiment. ^{1}H and ^{13}C chemical shifts were referenced with respect to DSS. Spectra were processed using topsin1.3 (Bruker Biospin) and T_1 and CP dynamic curves were fitted using the GOSA program [34].

3. Results

3.1. Screening of experimental conditions for the reconstitution of KpOmpA TM domain in lipid bilayers

Prior to the overexpression, purification and reconstitution of labeled *K. pneumoniae* outer membrane protein A (KpOmpA) for solid-state NMR (ssNMR) experiments, several reconstitution trials were conducted with non-labeled protein in order to optimize the conditions for the formation of proteoliposomes in terms of lipid composition, lipid-to-protein ratio (LPR) and dialysis buffer. The examination of negatively stained preparations by electron microscopy represents a suitable tool for this purpose because it enables rapid visualization and diffraction pattern-based analysis of the different preparations in order to identify regions of long-range ordered molecules in the bilayer. The goal of these pilot experiments was to establish conditions suitable for the arrangement of the protein in 2D crystals, which is beneficial for the ssNMR spectroscopic sensitivity and spectral resolution.

The reconstitution of KpOmpA into liposomes was achieved by slow dialysis-driven detergent removal. This is particularly important in the case of samples with low LPRs, in which the relatively large amount of protein must receive sufficient time for incorporation into the newly formed bilayers. Because the detergent used for the protein purification (Zwittergent 3–14) has a low critical micellar concentration (CMC ~ 0.012%), it is unsuitable for removal in this manner and therefore was exchanged for the high-CMC detergent *n*-octyl-β-D-glucopyranoside (OG, CMC ~ 0.7%), which is commonly used for the solubilization of *E. coli* OmpA [35]. The homogeneity of the micelle size was checked with gel filtration (data not shown) and the protein was found to be monomeric, as expected. Fig. 1E (lanes 1 to 4) shows an SDS PAGE gel of purified KpOmpA TM domain in 0.1% Zwittergent 3–14 (lanes 1 and 2) and in 2% OG (lanes 3 and 4), with the folded (lanes 1 and 3) and unfolded (heat-denatured, lanes 2 and 4) states visualized by the different migration of the bands [26]. The protein in 2% OG was then mixed with a particular lipid type and dialyzed following the procedure described in the materials and methods section to obtain proteoliposomes. The different trials were checked macroscopically, and then by electron microscopy.

We tested three types of lipids: DOPC, DMPC and *E. coli* polar lipid extract (PLE). These lipid types were chosen to comprise a variety of chain lengths and acyl chain saturation levels: the DOPC has long and unsaturated chains (18:1/18:1); the DMPC is shorter and saturated (14:0/14:0); and the "native-like" lipid mixture of the *E. coli* PLE contains different levels of lengths and saturation in its composition of L-α-phosphatidylethanolamine (67.0%), L-α-phosphatidylglycerol (23.2%) and cardiolipin (9.8%). The dialysis buffers tested encompassed different pH and ionic strengths. The range of LPRs investigated varied from 0.1 to 20 (w/w), corresponding to ~1 protein for between 3 and 600 lipid molecules. The results of these trials to determine appropriate conditions for the formation of proteoliposomes are reported in Fig. 1A.

We initially observed that samples contained high levels of macroscopically visible aggregated protein and/or vesicles, usually in conditions of lower pH and higher salt concentrations. The negative effect of low pH on sample quality is illustrated by the DOPC sample, which produced small and aggregated vesicles (Fig. 1B, pH 7.0). Based on the reconstitution trials, we concluded that, independently of the chosen LPR and ionic strength, the lower pH (HEPES at pH 7.0) does not appear to be as suitable for the formation of proteoliposomes as the higher pH (Tris at pH 8.5). This result agrees with previous observations that OmpA (as well as several other Omps) exhibits improved folding in slightly basic conditions [36,37]. We therefore excluded the samples at pH 7.0 from further experiments.

Because NMR is a demanding technique in terms of sensitivity, it is imperative to keep the LPR to a minimum in order to maximize the quantity of protein in the sample. We systematically observed aggregated samples at very low LPRs (i.e., 0.1–0.3 w/w) for any buffer condition, and to a lesser extent for smaller LPRs (i.e., 0.3 and 0.4) at higher pH and salt concentrations. As an illustration of the lack of sample homogeneity at low LPR values, Fig. 1C shows an aggregated DMPC sample with an LPR of 0.2 and a high pH (8.5). Such a low LPR (corresponding to ~6 lipid molecules per protein molecule), in the absence of 2D protein crystallization, threatens overall sample homogeneity and might lead to aggregation of at least part of the protein population. All of the lipids

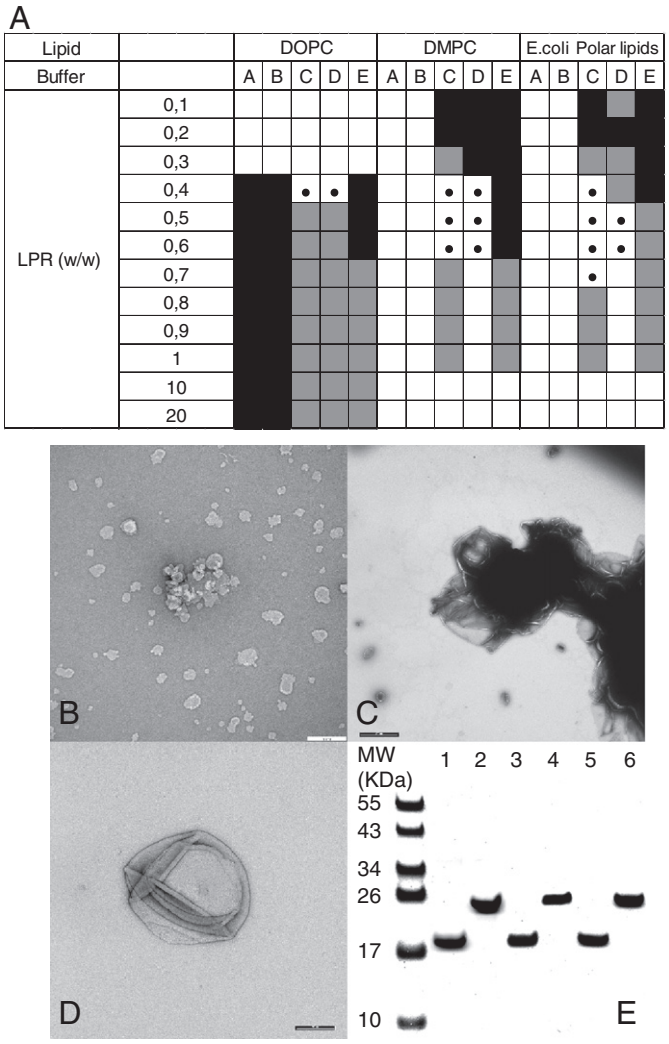

Fig. 1. Screening for the reconstitution of KpOmpA TM domain in lipid vesicles. (A) Summary of experimental conditions screened for the reconstitution of KpOmpA in lipid vesicles. Positive hits are identified with a white box and a black dot. Black boxes represent rejected conditions in which the samples were heavily aggregated. Gray boxes represent intermediate conditions: sample exhibiting moderate aggregation and/or presenting a threat to the overall homogeneity (too low LPR) or to the efficiency of centrifugation (too high LPR). Reconstitution buffers are labeled from A to E: *Buffer A*, 20 mM Hepes (pH 7.0), 140 mM NaCl; *Buffer B*, 20 mM Hepes (pH 7.0), 300 mM NaCl; *Buffer C*, 20 mM Tris–HCl (pH 8.5), 100 mM NaCl; *Buffer D*, 20 mM Tris–HCl (pH 8.5), 140 mM NaCl; *Buffer E*, 20 mM Tris–HCl (pH 8.5), 300 mM NaCl. (B–D) Electron micrographs of negatively-stained KpOmpA-containing vesicles with different conditions (the scale bar is 200 nm); (B) the lower pH reduces the sample quality, resulting in small, aggregated vesicles when the protein is reconstituted at LPR of 0.4 (w/w) in DOPC (20 mM HEPES at pH 7.0, 140 mM NaCl). (C) Sample aggregation at LPR of 0.2 (w/w) in DMPC (20 mM Tris at pH 8.5, 100 mM NaCl). (D) Vesicle with reconstituted KpOmpA TM domain at LPR of 0.5 (w/w) in *E. coli* polar lipid extract (PLE, 20 mM Tris at pH 8.5, 140 mM NaCl). (E) Coomassie stained SDS PAGE gel of KpOmpA TM domain in different environments. The KpOmpA TM domain purified in 0.1% Zwittergent 3–14 (lanes 1 and 2), in 2% OG after detergent exchange (lanes 3 and 4) and in *E. coli* PLE after reconstitution for ssNMR experiments (lanes 5 and 6). The aliquots on lanes 1, 3 and 5 represent the native fold of the β-barrel, whereas those on lanes 2, 4 and 6 are heat-denatured (100 °C, 5 min) and the protein bands appear at their expected positions (~23.4 kDa) from the marker ladder on the left lane.

tested produced usable samples in conditions where neither the pH nor the LPR were too low. An LPR of 0.5 (w/w, corresponding to about 15 lipids per protein molecule) is acceptable for our purposes, as this condition significantly reduces the probability of protein aggregation and still enables the preparation of a sample for NMR containing more than 20 mg of protein. For example, Fig. 1D demonstrates the homogeneity of a typical sample at this LPR value in *E. coli* PLE. Control 1D and 2D PDSD ^{13}C NMR spectra were performed at LPR = 1 and no difference was observed with those at LPR = 0.5. Therefore, samples with an LPR of 0.5 were selected for use in ssNMR experiments, and samples with an LPR above this value and a high salt concentration were discarded (see gray squares in Fig. 1A).

Further examination of the different pilot samples led to the conclusion that the most suitable lipid type for our purposes was the *E. coli* PLE, although we concluded that all three lipids tested were appropriate for the dialysis-based reconstitution of KpOmpA in these conditions. However, the substantially longer chains of DOPC (18:1/18:1) form bilayers with a thickness (~5.5 nm at room temperature [38]) that does not correlate closely with the section of the protein known to be embedded in the membrane (~2 nm), and this hydrophobic mismatch could result in altered dynamics at the interface between the β-barrel and the loops. Conversely, DMPC has the disadvantage of a higher gel to fluid phase transition temperature (~23 °C). However, the *E. coli* PLE is usable at room temperature and should mimic the protein's natural environment in the outer membrane of Gram-negative bacteria in terms of polar-head composition.

Finally, in the range of 100–300 mM NaCl, no significant influence of the ionic strength on protein reconstitution was observed by electron microscopy. The electron diffraction experiments provided no evidence, in any sample preparations, of the existence of 2D-crystals, such as those observed with OmpG [39]. The monomeric nature of KpOmpA and the geometrical symmetry of its β-barrel, combined with the lack of structural features provided by the loops [40] presumably contribute to this lack of long-range 2D order. Based on the screening of

experimental conditions, we finally decided to reconstitute the KpOmpA TM domain in *E. coli* PLE at an LPR of 0.5 (w/w) and in buffer C (i.e. pH 8.5) without salts, in order to prevent sample heating during the NMR experiments. The large-scale proteoliposome preparation for NMR spectroscopy was first performed with unlabeled protein and the full-scale sample was further characterized by sucrose gradient centrifugation. The gradient centrifugation produced a single, well-defined band at ~45–47% sucrose that was subsequently analyzed with protein and phospholipid colorimetric assays. The LPR of the isolated band was confirmed to be ~0.5 (w/w). The proteoliposomes generated, regardless of their variation in size and aggregation state, possess the same LPR, as demonstrated by the single band in the sucrose gradient centrifugation. The folded and unfolded states of the reconstituted protein were also verified with SDS PAGE (Fig. 1E, lanes 5 and 6).

3.2. ssNMR characterization of KpOmpA TM domain in E. coli PLE vesicles

Fig. 2A shows the 2D (^{13}C, ^{13}C) proton-driven spin diffusion (PDSD) correlation spectrum of (U–^{13}C, ^{15}N)-KpOmpA/PLE proteoliposomes (LPR of 0.5, w/w) recorded at 20 °C with 40 ms mixing time. Under these conditions, the lipid bilayer is fluid and the ssNMR spectrum is dominated by the intraresidue correlation network of the protein. Characteristic one- to three-bond intraresidue CC connectivities were identified for several amino-acid types, including Thr, Ser, Pro, Ala and Ile (Fig. 2A, boxes). As an example, the complete correlation network between the α, β and γ2 carbons of two Thr residues is shown (solid and dashed lines). According to standard amino acid-peak positions [41] and the overall correlation pattern, the PDSD spectrum of KpOmpA reflects predominantly β-sheet and random coil protein segments, in accordance with the topological profile of the protein in detergent micelles. Spectral resolution is given by ^{13}C line-widths of 0.6–0.9 ppm for isolated resonances (Fig. 2B). This is in agreement with the literature, where the typical ^{13}C line-widths observed by ssNMR vary from 0.5 to 0.7 ppm for small (<100 residues) uniformly [^{13}C, ^{15}N]-labeled proteins in micro-crystalline form [42–44] and seven-helix receptors (NpSRII) in native membranes [45], respectively. Although the spectral resolution is high, the CC correlation spectrum is characterized by a significant resonance overlap resulting from the high frequency of occurrence of particular residue types in β-sheet TM segments (e.g., Leu and Val) and loop regions (e.g., Ser and Arg), which significantly hampered the resonance assignment procedure and residue-specific analysis. We thus compared our results with data obtained using the perdeuterated KpOmpA TM domain in DHPC micelles (BMRB accession code 15651). Prior to chemical-shift analysis, $^{13}C^{\alpha}/C^{\beta}$ chemical shifts were corrected for the ^{2}H-isotope effect as described by Venters et al. [46]. The intraresidue correlation network was then calculated from the corrected solution NMR chemical shifts and the prediction was overlaid with the 2D PDSD spectrum of KpOmpA (Fig. S1). A remarkable agreement between the solution NMR chemical shifts and the overall CC correlation pattern of KpOmpA was observed, suggesting that the global fold of the protein in DHPC micelles is well preserved in PLE bilayers. Notably, isolated backbone resonances corresponding to Thr, Ser, Val, Ala and Leu residues within KpOmpA TM segments were readily observed in the vicinity of peak positions predicted from solution NMR chemical shifts (Fig. S1, solid squares). In contrast, significant deviations between ssNMR and solution NMR data were observed for a set of residues located in the unstructured N-terminal extremity (Ile3, Ile7) and in the first (Asn63 and Pro64) and second (Pro103 and Ile104) periplasmic turns, suggesting that conformational and/or dynamical changes may occur around these residues in the lipid environment. Finally, correlations corresponding to residues within extracellular loops were also visible, suggesting a reduced mobility within unstructured protein segments in the lipid environment (Fig. S1, dashed squares).

The contribution of the unstructured extracellular loops to the KpOmpA PDSD spectrum was investigated in more detail by examining the spectral region of the C^{α}–C^{β} resonances of the Thr and Ser residues (Fig. 3A), which are well-distributed within the extracellular loops (from L1 to L4) and β-sheet TM segments (TM1, TM3-TM8) of the protein (Fig. 3C and D). Taking into account the number of residues forming the cross-peaks, the intensity is systematically smaller when the residue is located in the loop than in the β-sheet (Fig. 3B). Considering the Thr residues, the intensity of the C^{β}–C^{α} cross-peak is much smaller for the five residues constituting the loops (T-33,47,130,174,177) compared with the seven residues of the β-barrel (T-18,97,105,112,139, 154,159). Similarly, the signals of Ser residues within the loops is smaller compared with Ser signals in the β-sheet protein segments, and only

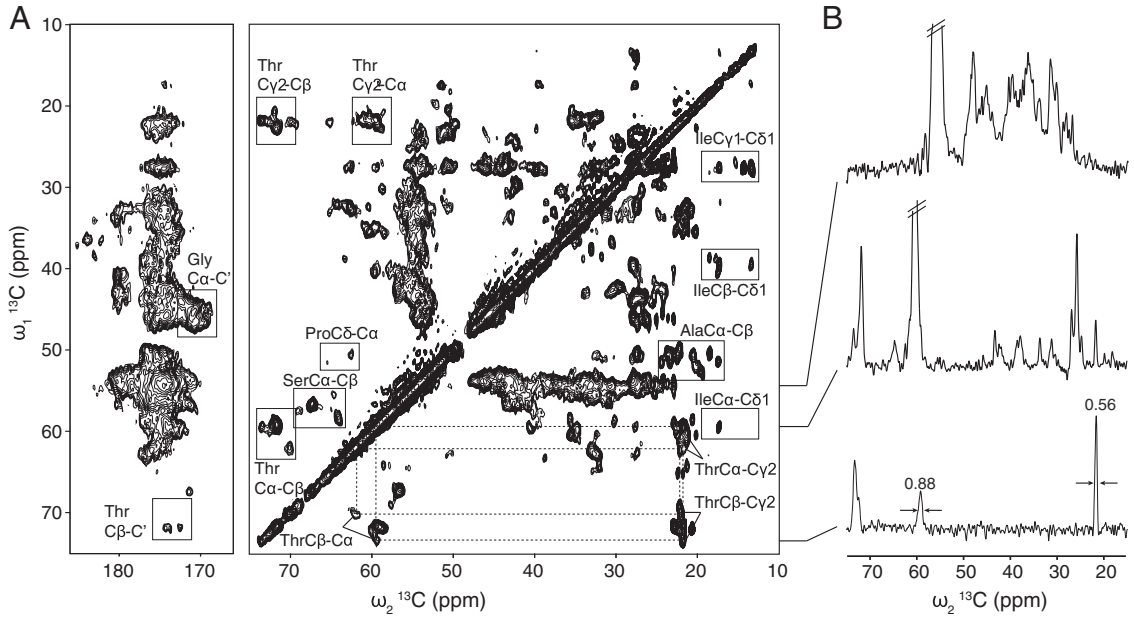

Fig. 2. (A) Carbonyl and aliphatic regions of the 2D ^{13}C, ^{13}C PDSD correlation spectrum (40 ms mixing time) recorded on reconstituted (U–^{13}C, ^{15}N)-labeled KpOmpA TM domain in *E. coli* polar lipid extract (PLE) vesicles at a sample temperature of 20 °C with MAS 12 kHz and a proton Larmor frequency of 700 MHz. Amino acid-specific assignments are indicated. Dashed lines indicate the characteristic intraresidue CC connectivities of Thr within β-sheet and loop protein regions, respectively. (B) Series of 1D slices extracted from the 2D ^{13}C, ^{13}C PDSD correlation spectrum at different ω_1 ^{13}C frequencies. The carbon line-widths of the Thr C^{α} and CH_3 resonances are indicated in ppm. The NMR samples typically contained 22 mg of protein, 11 mg of lipids and 17 mg of water (lipid/protein molar ratio = 15/1).

three of eight assigned Ser residues are located into the β-barrel. This difference in the intensities is obviously induced by different dynamic regimes in two distinct moieties of the protein: the TM domain and the loops. Thus the CP + PDSD transfer schemes select a subset of the loops' resonances, attenuating but not completely suppressing the most mobile signals arising from the loop region. Further characterization of these remaining resonances is presented in the following section.

3.3. Dynamics of KpOmpA over different NMR time scales

The rotational diffusion correlation times of membrane embedded proteins are much slower than for small soluble proteins (typically above microseconds [47]) and NMR relaxation rates are thus sensitive to dynamics up to microsecond timescales. Various ssNMR methods have been developed to measure R1, R1ρ, and heteronuclear NOEs [48–50]. Using extended model free formalism, spectral density functions could be expressed in terms of order parameters and correlations times for slow and fast motions and dynamics time scale could be determined [51,52].

To investigate the different degrees of molecular mobility within the KpOmpA TM domain, we recorded a series of three ^{13}C-detected 1D spectra using different excitation schemes (i.e., direct ^{13}C excitation, ^{1}H–^{13}C refocused-INEPT and ^{1}H–^{13}C CP, Fig. 4). The direct ^{13}C excitation spectrum (Fig. 4A) constitutes the reference spectrum, in which signal intensities are most directly related to the number of carbons. Accordingly, Thr C^{β} resonances revealed similar peak intensities for residues within the β-sheet (B peak at 71.8 ppm, 7 Thr) and random coil segments (L peak at 70 ppm, 5 Thr). In contrast, the ^{1}H–^{13}C INEPT spectrum (Fig. 4C) displays signal intensity only at 70 ppm, which arises from the loop regions. Indeed, the ^{1}H–^{13}C INEPT type experiments employ a magnetization transfer step mediated by ^{1}H–^{13}C scalar (through-bond) coupling. This coupling takes a few milliseconds to establish, during which time the magnetization transfer mediated by strong dipolar couplings vanishes due to fast R_2 relaxation for rigid segments. Therefore, only protein segments undergoing fast (ns) isotropic motions persist in the INEPT spectrum. In contrast, CP-based experiments filter out magnetization from spins in fast motional regimes, and thus signals from rigid protein regions dominate the spectrum. As expected,

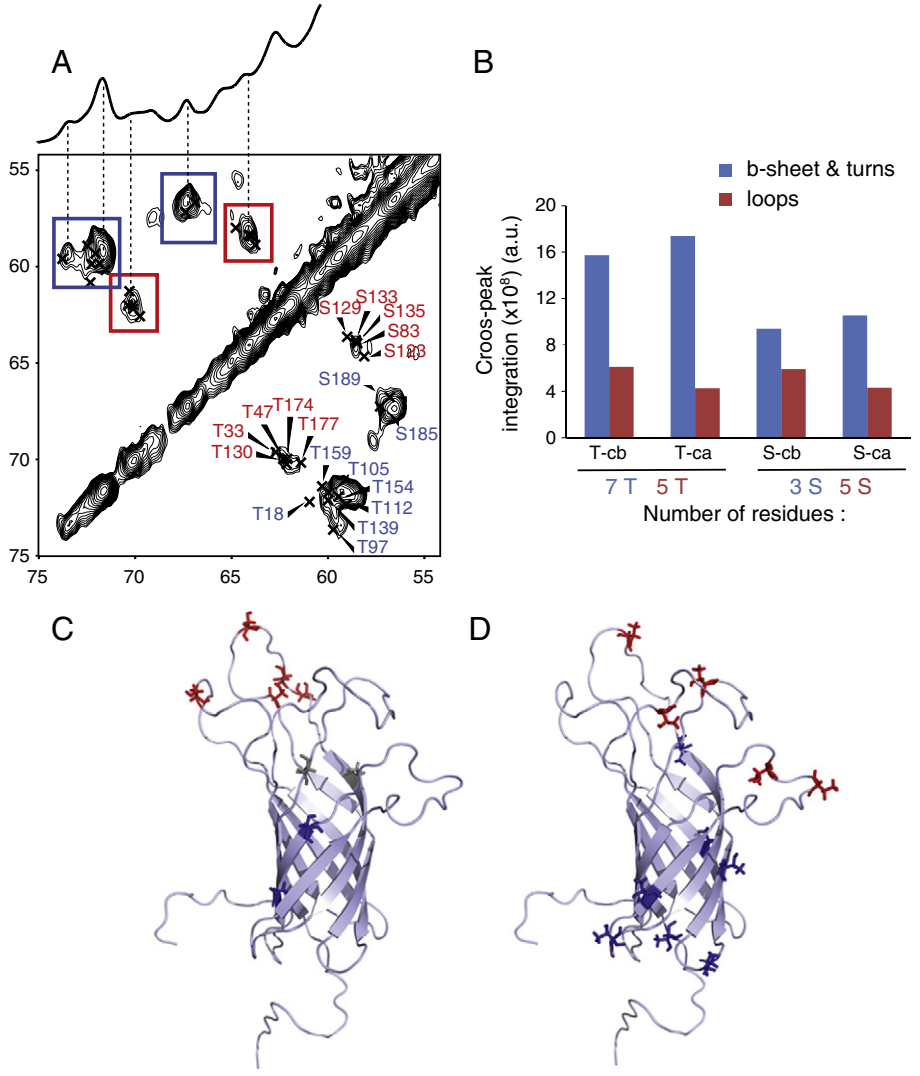

Fig. 3. (A) Selected region of the 2D ^{13}C, ^{13}C PDSD correlation spectrum showing backbone C^{β}–C^{α} correlations of the Thr and Ser residues of KpOmpA TM domain. Solution NMR assignments are indicated when available. Open rectangles represent spectral regions used for signal integration, expected correlations were obtained from available solution NMR chemical shifts of KpOmpA TM domain (BMRB 15651 [9]) after correction due to ^{2}H isotope effect. (B) Integrations of spectral regions corresponding to Thr and Ser residues within random-coil (red bars) and β-sheet-like (blue bars) protein segments plotted onto the number of residues. (C) Distribution of Ser residues within KpOmpA TM domain (PDB ID: 2K0L). (D) Distribution of Thr residues within KpOmpA TM domain. For (C) And (D) the color code is: residues within β-sheet TM and turns segments are in blue, those within the extracellular loops are in red. Two unassigned residues are labeled in dark gray. (For interpretation of the references to color in this figure legend, the reader is referred to the web version of the article.)

in the CP spectrum an intense peak was observed at 71.8 pm, characteristic of rigid protein TM segments (Fig. 4B). Interestingly, a signal of lower intensity is still observed at 70 ppm in the CP spectrum, indicating the presence of restricted protein motions in the unstructured extracellular loops. These results suggest the presence of multiple motional regimes within the extracellular loops of KpOmpA.

Next, we measured the ^{13}C spin–lattice relaxation time (T_1) of the C^{α} and C^{β} of the Ser and Thr residues from 2D PDSD ^{13}C–^{13}C spectra by incorporating a longitudinal relaxation delay between the CP and the first ^{13}C time evolution. ^{13}C T_1 relaxation is dominated by the C-H dipolar interaction mechanism and depends on the motional regime. The results of this experiment can only be discussed qualitatively, because they are averaged over several overlapping residues and because of the contribution of proton driven carbon-carbon.

spin diffusion [53]. We systematically observed shorter T_1 values for the residues constituting the loops compared with those in the β-sheets (Fig. 5A). For example, for the Thr C_{α} carbons: $T_{1\text{-}C\alpha} = 0.46 \pm 0.16$ s in the loops, and $T_{1-C\alpha} = 1.14 \pm 0.07$ s in the β-barrel. For the Ser C_{α} carbons: $T_{1\text{-}C\alpha} = 0.32 \pm 0.18$ s in the loops and $T_{1-C\alpha} = 1.63 \pm 0.30$ s in the β-barrel. This result reveals that there are increased motions in the loops around the ^{13}C Larmor frequency, because the R_1 longitudinal relaxation rate ($1/T_1$) is enhanced by these motions, with characteristic times in the nanosecond and sub-nanosecond range.

The dynamics of the CP were examined by using contact times from 50 μs to 8 ms on the 2D ^{13}C–^{13}C spectrum. The CP dynamics are described most simply by a two-stage model. The "build-up" phase starts at very short contact times and is caused by the initial CP transfer from ^{1}H to the closest ^{13}C via ^{1}H–^{13}C dipolar interactions. This CP transfer is usually characterized by a constant time, called T_{CP}. This initial phase is followed by a "decay" phase caused by the relaxation of the spin-locked ^{1}H, with a characteristic time $T_{1\rho}$ [32]. We observed that T_{CP} values for each residue and carbon type are systematically longer when the Ser and Thr residues are located in a loop rather than in the β-barrel (Fig. 5B). For example, T_{CP} for the Thr C^{β} is equal to 51 ± 10 μs in the β-barrel and increases to 108 ± 14 μs in the loops. Similarly, T_{CP} for the Ser C^{β} is 26 ± 10 μs in the β-barrel and 82 ± 14 μs in the loops.

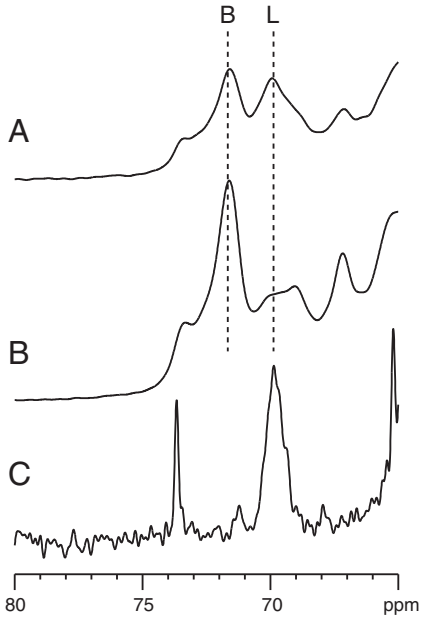

Fig. 4. 1D proton decoupled, ^{13}C-detected MAS NMR spectra of reconstituted (U–^{13}C, ^{15}N)-labeled KpOmpA in *E. coli* PLE vesicles recorded at a MAS frequency of 12 kHz and a sample temperature of 20 °C. (A) Direct excitation recorded with a 90° pulse on ^{13}C and accumulated 2 K scans; (B) cross-polarization (CP) transfer MAS recorded with a CP contact time of 400 μs, with 2 K scans; (C) refocused-INEPT excitation recorded with 12 K scans. NMR chemical shifts of Thr C^{β} resonances characteristic of β-sheet TM and random coil protein regions (loops) are labeled B and L, respectively.

This slower polarization transfer in the loop regions is caused by partial averaging of the ^{1}H–^{13}C dipolar interaction by the greater mobility of the loops in the sub-microsecond range.

The $T_{1\rho}$ values extracted from the 2D CP dynamic experiment analysis vary from 1.6 to 3.6 ms depending on the carbon and residue types (Fig. 5C). These values are in agreement with values reported for proteorhodopsin in a lipid environment [54]. For the analysis of the spin–lattice relaxation in the laboratory frame (T_1) analysis, the comparison was restricted to $T_{1\rho}$ values for the same carbon in two distinct secondary structure elements. In these conditions, both the C^{α} and C^{β} of the Thr residues exhibited larger $T_{1\rho}$ values for residues in the β-barrel compared with the loops (i.e., Thr C^{α} $T_{1\rho} = 3.72 \pm 0.48$ ms and 1.75 ± 0.29 ms, respectively). The faster average $R_{1\rho}$ relaxation rate in the loops is probably related to the Thr localization: three of five Thr residues constituting the loops (T33, T174 and T177, in orange in Fig. 6) are located in the region of the loops that undergo restricted mobility with motions in the ms to μs range, which are known to be important for $R_{1\rho}$ relaxation. In contrast with the Thr residues, the C^{α} of the Ser residues present in the loops exhibited less efficient $R_{1\rho}$ relaxation and the majority of the Ser residues participating in the loop cross-peak are located in the C-terminal region of L3 (S129, S133 and S135), which is highly flexible. These Ser residues are expected to be dominated by fast isotropic motions, outside the millisecond to microsecond range, and therefore to give less efficient $R_{1\rho}$ relaxation.

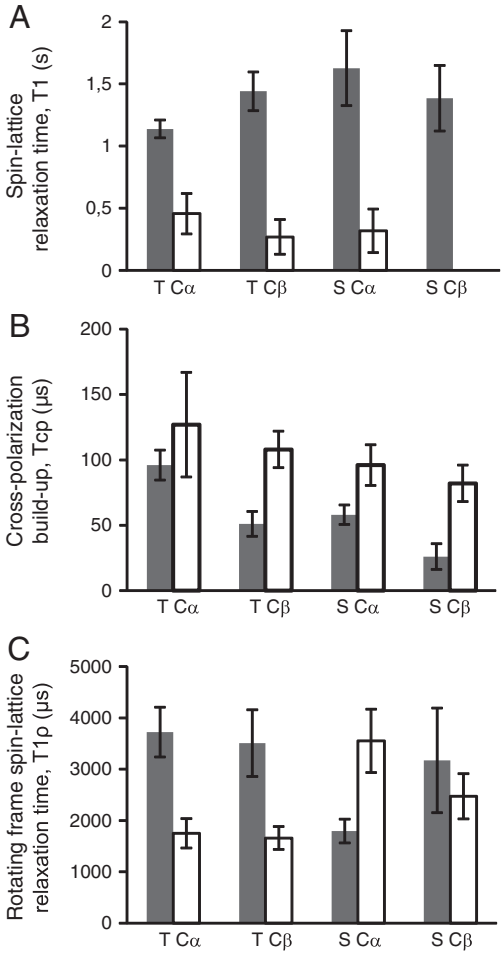

Fig. 5. (A) ^{13}C spin–lattice relaxation time (T_1) of C^{α} and C^{β} of serine (S) and threonine (T) residues, (B) and (C) correspond respectively to the cross-polarization build-up (T_{CP}) and proton spin–lattice relaxation time in the rotating frame ($T_{1\rho}$) determined from the cross-polarization dynamics. Gray bars correspond to carbons within β-sheet TM and turns segments; white bars correspond to carbons within the extracellular loops.

4. Discussion

The structure and dynamics of KpOmpA have been studied by NMR in two distinct environments: in DHPC micelles [9]; and in *E coli* polar lipid extract (PLE) proteoliposomes (present work). Careful optimization of the reconstitution protocol has permitted the preparation of homogeneous liposomes with a large lipid to protein ratio (LPR = 0.5, typically 22 mg protein for 11 mg lipid, molar ratio of 1 to 15) that is compatible with a detailed ssNMR characterization, which is quite demanding in terms of sensitivity. Electron microscopy demonstrated the samples to be homogeneous under these conditions, with no indication of 2D crystallization of the protein in the lipid bilayer planes. 2D PDSD showed good resolution of the ^{13}C resonances and significant similarity between ^{13}C chemical shifts in bilayers and in DHPC micelles, revealing that the overall fold of the protein is identical in both environments. 2D PDSD acquired at a LPR of 1 and 0.5 were identical, suggesting that the molecular crowding did not affect much the protein dynamics in this range of protein concentration. The lipid to protein ratio in Gram negative bacteria outer membranes is estimated to in the 0.5 to 1 range [55–57], i.e. not so far from our experimental conditions. The KpOmpA TM domain has been demonstrated to exhibit ns- to μs-timescale molecular motions when embedded in detergent micelles [9]. Heteronuclear ^{1}H–^{15}N NOE relaxation of the backbone ^{15}N spins was used to probe the picosecond to nanosecond dynamic fluctuations of individual N – H bonds, chemical exchange line-broadening of the backbone amide resonances were sensitive to microsecond to millisecond backbone motions, and $^{2}H_2O/H_2O$ solvent exchange experiments were used to probe slower dynamic processes (seconds to days). A mobility gradient was observed, from the rigid β-barrel embedded in the hydrophobic core of the micelles to the disordered and highly dynamic loops. At the boundary of these two regions (i.e., the interface region), residues exhibited intermediate motions with characteristic times of micro- to milliseconds, as reflected by the extended conformational exchange-induced line broadening. In most of the β-barrel-to-loop interface, and despite the large heteronuclear NOE values that reflect an ordered structure, residues belonging to the β-barrel (Fig. 6, squares in orange) exhibit conformational exchange, characterized by line-broadening at different temperatures and static magnetic field strengths. This conformational exchange is propagated toward the loops, in which regions the induced line-broadening increased to the extent that it hampered the assignment of resonances (Fig. 6, orange circles filled with gray). Moreover, restricted mobility was measured from heteronuclear NOE values (average value of 0.6 ± 0.1) for residues with random coil chemical shifts from S28 to N38 in L1, from D122 to Y127 in L3 and for the entire L2 and L4 loops (Fig. S3 in [9]).

In lipid bilayers, KpOmpA dynamics had to be studied by ssNMR approaches, such as T_2-filter, dipolar- and scalar-based polarization transfer, to identify mobile and static moieties [54,58]. Several approaches to assess internal dynamics in a site-specific manner have been reported, such as ^{15}N spin–lattice relaxation rates and averaged dipolar and/or CSA interactions [49,50,59]. However, due to the relatively large molecular weight of KpOmpA, a residue type specific approach was used, with observations focused on the Thr and Ser resonances, which are well-distributed within the 3D fold, as shown in Fig. 3. All of the evidence described in the results section indicates that KpOmpA has an identical structure and dynamics in micelles and in lipid bilayers. The 2D PDSD experiments demonstrate that the carbon chemical shifts are highly similar in both environments, as shown in Fig. S1. Ser and Thr are well-distributed throughout the β-sheet and random coil environments. The resonances from residues in the β-barrel possess all of the characteristics of rigid segments; for example, shorter T_{CP} build-up rates, the absence of signal in INEPT-based excitation and longer T_1 relaxation times. Loops L2 and L4, and the N-terminal parts of loops L1 and L3 are subjected to millisecond to microsecond motions (as revealed by longer T_{CP} and shorter $T_{1\rho}$ times for Thr signals), whereas the C-terminal part of loops L1 and L3 are subjected to motions of higher frequency and/or higher amplitude (as revealed by the Thr signals observed in an INEPT excitation scheme, and by the longer $T_{1\rho}$ of the Ser 129, 133, 135 resonances in L3).

Taken together, the differences observed in the behavior of the Ser and Thr residues suggest that the dynamics with an intermediate time scale that were observed for KpOmpA in micelles [9] persist at the

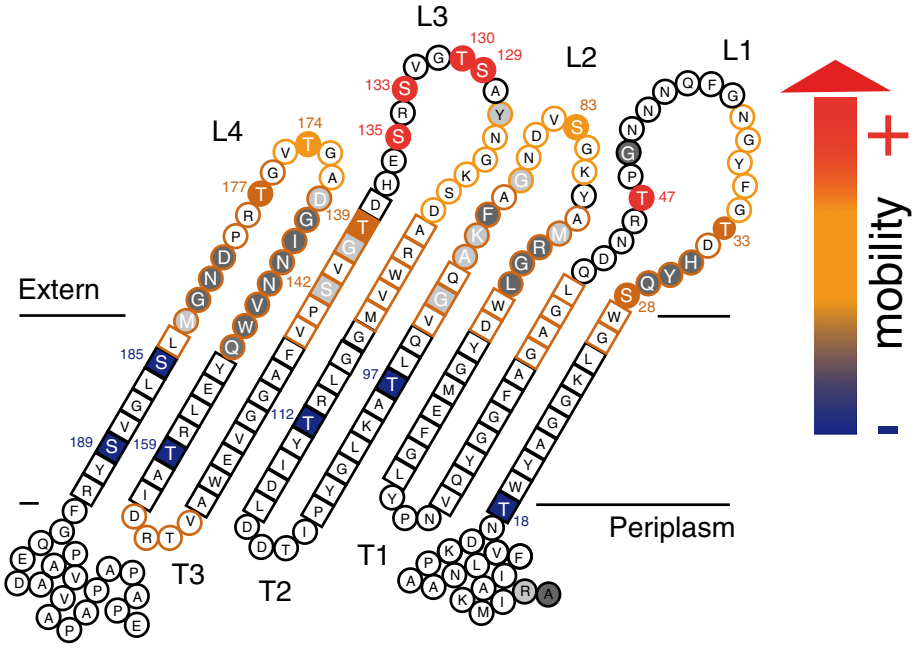

Fig. 6. Dynamics of KpOmpA TM domain in lipid bilayers. Topological representation of KpOmpA TM domain (PDB ID: 2K0L) illustrating residue-specific mobility within distinct protein segments. Residues within β-sheet and random coil regions are represented by squares and circles, respectively. Amino acids are given in single-letter notation. In both DHPC micelles and *E. coli* polar lipid extract bilayers, residues that experience fast isotropic motions are colored in red and rigid protein segments are colored in blue. Residues that exhibit restricted mobility in DHPC micelles are highlighted; they correspond to residues in conformational exchange (dark orange) and characterized by ^{1}H–^{15}N NOEs at 0.6 ± 0.1 (light orange). Unassigned residues are colored in gray.

membrane interface in presence of lipid bilayers, where there are specific constraints such as lipid lateral pressure and membrane strain curvature. This conservation of dynamics in different conditions could be related to the amino acid composition of the protein at the interface. Indeed, it has been demonstrated that the mutation of Trp residues to Phe in OmpA from *E. coli* reduces the conformational exchange phenomena [19] and allows the assignment of more residues at the interface. However, no conformational exchange processes probed by relaxation dispersion experiments in the millisecond to microsecond range were revealed for any of the observable residues of *E. coli* OmpA, suggesting the absence of global backbone conformational changes [60]. Such global changes have been reported for PagP in micelles [61].

The C-terminal halves of L1 and L3 in KpOmpA exhibit typical loop behavior, with random coil chemical shifts, few unassigned residues and fast isotropic dynamics (Fig. 6). Approximately half of the residues in L2 and L4 remain unassigned, due to millisecond to microsecond conformational exchange processes. These exchange phenomena seem to propagate up to the center of the loops that presents a restricted mobility. Interestingly, the alignment of KpOmpA with its *E. coli* homolog shows a high level of similarity between their respective loops L2 and L4, whereas the other two loops (L1 and L3) are more diverse (Supplementary Fig. 2). It is unclear whether the conservation of L2 and L4 is the result of evolutionary pressure, similar to that exerted on the conserved β-barrels of these molecules. The structural importance of the extracellular loops is still discussed. Datta et al. [62] suggested that inter-loop interactions are critical for maintaining the 3D structure of OmpA from *E. coli*, whereas Koebnik claimed that the structural integrity of the protein is entirely attributed to the β-barrel and turns region, because loop-truncated mutants did not exhibit thermal instability [40]. Surprisingly, in the same study by Koebnik et al., these highly disordered loops were not digested by subtilisin, provided that the full complement of loops was present, although the truncated mutants were more susceptible to digestion. We also observed (data not shown) for KpOmpA that Lysine-C endoprotease is not able to cleave the loops, despite the fact that there are two Lys residues in L2 and one in the L3 N-terminal half. Hence, our NMR data correlates well with the results of biochemical experiments. It was previously reported that *E. coli* OmpA and KpOmpA are necessary for invading brain endothelial cells [63] and bronchial epithelial cells [64], respectively, and that both proteins participate in bacterial survival in macrophages. A detailed study with a variety of mutants established the importance of the different loops of *E. coli* OmpA during these immunological processes [65,66]. L2 contributes to bacterial survival in dendritic cells and polymorphonuclear lymphocytes, as well as influencing the immune response by binding, together with the more conserved L4, to the complement pathway regulator C4bp. Interestingly, the loop mutants that exhibited reduced invasiveness were those with altered amino acids in the interfacial, less dynamic regions of L2 and L4, as well as the less flexible segment of L1 emanating from the β-barrel immediately after the first β-sheet (Fig. 6).

Taken together, these data suggest that the reduced mobility in certain loop areas correlates with their level of evolutionary conservation (highest in L4) and their propensity for involvement in bacteria invasion. This could be explained either by the contribution of these regions to the stability of the underlying, and similarly well-conserved β-barrel and/or by their function as "antigen presenting" segments, responsible for proper positioning of the host receptor-binding motifs found in the highly disordered extremities of the loops. The residues found "on top" of the loops are both the most variable and the most mobile. More precisely, our observations in solution and ssNMR indicate that two regions of loop L1 (from G39 to T47) and of loop L3 (from A128 to E136) are the most mobile segments of the outer surface of KpOmpA.

Acknowledgment

These studies and the IPBS NMR equipment were financed by the French Research Ministry, CNRS, Université Paul Sabatier, the Région Midi-Pyrénées and European structural funds. The NMR data were acquired on the spectrometers of the PICT-IBiSA national facility. The research leading to these results has received funding from the European Community's Seventh Framework Program FP7/2007-2013 under grant agreement no. 211800, and from the European Drug Initiative on Channels and Transporters grant HEALTH-F4-2007-201924. Deborah Gater is acknowledged for the final reading of the manuscript.

Appendix A. Supplementary material

Supplementary data to this article can be found online at http://dx.doi.org/10.1016/j.bbamem.2012.05.004.

References

[1] E. Wallin, G. von Heijne, Genome-wide analysis of integral membrane proteins from eubacterial, archaean, and eukaryotic organisms, Protein Sci. 7 (1998) 1029–1038.
[2] G.C. Terstappen, A. Reggiani, In silico research in drug discovery, Trends Pharmacol. Sci. 22 (2001) 23–26.
[3] P.J. Judge, A. Watts, Recent contributions from solid-state NMR to the understanding of membrane protein structure and function, Curr. Opin. Chem. Biol. 15 (2011) 690–695.
[4] J.H. Chill, F. Naider, A solution NMR view of protein dynamics in the biological membrane, Curr. Opin. Struct. Biol. 21 (2011) 627–633.
[5] L.K. Tamm, B.Y. Liang, NMR of membrane proteins in solution, Prog. Nucl. Magn. Reson. Spectrosc. 48 (2006) 201–210.
[6] H.J. Kim, S.C. Howell, W.D. Van Horn, Y.H. Jeon, C.R. Sanders, Recent advances in the application of solution NMR spectroscopy to multi-span integral membrane proteins, Prog. Nucl. Magn. Reson. Spectrosc. 55 (2009) 335–360.
[7] A. McDermott, Structure and dynamics of membrane proteins by magic angle spinning solid-state NMR, Annu. Rev. Biophys. 38 (2009) 385–403.
[8] A. Naito, Structure elucidation of membrane-associated peptides and proteins in oriented bilayers by solid-state NMR spectroscopy, Solid State Nucl. Magn. Reson. 36 (2009) 67–76.
[9] M. Renault, O. Saurel, J. Czaplicki, P. Demange, V. Gervais, F. Lohr, V. Reat, M. Piotto, A. Milon, Solution state NMR structure and dynamics of KpOmpA, a 210 residue transmembrane domain possessing a high potential for immunological applications, J. Mol. Biol. 385 (2009) 117–130.
[10] T.N. Nguyen, P. Samuelson, F. Sterky, C. Merle-Poitte, A. Robert, T. Baussant, J.F. Haeuw, M. Uhlen, H. Binz, S. Stahl, Chromosomal sequencing using a PCR-based biotin-capture method allowed isolation of the complete gene for the outer membrane protein A of *Klebsiella pneumoniae*, Gene 210 (1998) 93–101.
[11] P. Jeannin, B. Bottazzi, M. Sironi, A. Doni, M. Rusnatl, M. Presta, V. Maina, G. Magistrelli, J.F. Haeuw, G. Hoeffel, N. Thieblemont, N. Corvaia, C. Garlanda, Y. Delneste, A. Mantovani, Complexity and complementarity of outer membrane protein a recognition by cellular and humoral innate immunity receptors, Immunity 22 (2005) 551–560.
[12] C. March, D. Moranta, V. Regueiro, E. Llobet, A. Tomas, J. Garmendia, J.A. Bengoechea, *Klebsiella pneumoniae* outer membrane protein A is required to prevent the activation of airway epithelial cells, J. Biol. Chem. 286 (2011) 9956–9967.
[13] S.G. Smith, V. Mahon, M.A. Lambert, R.P. Fagan, A molecular Swiss army knife: OmpA structure, function and expression, FEMS Microbiol. Lett. 273 (2007) 1–11.
[14] E. Sugawara, H. Nikaido, Pore-forming activity of OmpA protein of *Escherichia coli*, J. Biol. Chem. 267 (1992) 2507–2511.
[15] A. Negoda, E. Negoda, R.N. Reusch, Resolving the native conformation of *Escherichia coli* OmpA, FEBS J. 277 (2010) 4427–4437.
[16] S.G.J. Smith, V. Mahon, M.A. Lambert, R.P. Fagan, A molecular Swiss army knife: OmpA structure, function and expression, FEMS Microbiol. Lett. 273 (2007) 1–11.
[17] A. Pautsch, G.E. Schulz, Structure of the outer membrane protein A transmembrane domain, Nat. Struct. Biol. 5 (1998) 1013–1017.
[18] A. Pautsch, G.E. Schulz, High-resolution structure of the OmpA membrane domain, J. Mol. Biol. 298 (2000) 273–282.
[19] A. Arora, F. Abildgaard, J.H. Bushweller, L.K. Tamm, Structure of outer membrane protein A transmembrane domain by NMR spectroscopy, Nat. Struct. Biol. 8 (2001) 334–338.
[20] K. Cox, P.J. Bond, A. Grottesi, M. Baaden, M.S. Sansom, Outer membrane proteins: comparing X-ray and NMR structures by MD simulations in lipid bilayers, Eur. Biophys. J. 37 (2008) 131–141.
[21] R.S. Cantor, Lipid composition and the lateral pressure profile in bilayers, Biophys. J. 76 (1999) 2625–2639.
[22] J.T. Groves, The physical chemistry of membrane curvature, Nat. Chem. Biol. 5 (2009) 783–784.
[23] P. Garidel, C. Johann, A. Blume, Thermodynamics of lipid organization and domain formation in phospholipid bilayers, J. Liposome Res. 10 (2000) 131–158.
[24] D. Fourel, A. Bernadac, J.M. Pages, Involvement of exposed polypeptide loops in trimeric stability and membrane insertion of *Escherichia-coli* Ompf Porin, Eur. J. Biochem. 222 (1994) 625–630.
[25] A. Basle, G. Rummel, P. Storici, J.P. Rosenbusch, T. Schirmer, Crystal structure of osmoporin OmpC from *E. coli* at 2.0 Å, J. Mol. Biol. 362 (2006) 933–942.
[26] K. Nakamura, S. Mizushima, Effects of heating in dodecyl sulfate solution on the conformation and electrophoretic mobility of isolated major outer membrane proteins from *Escherichia coli* K-12, J. Biochem. 80 (1976) 1411–1422.

[27] J.L. Rigaud, M.T. Paternostre, A. Bluzat, Mechanisms of membrane protein insertion into liposomes during reconstitution procedures involving the use of detergents. 2. Incorporation of the light-driven proton pump bacteriorhodopsin, Biochemistry 27 (1988) 2677–2688.
[28] O.H. Lowry, N.J. Rosebrough, A.L. Farr, R.J. Randall, Protein measurement with the Folin phenol reagent, J. Biol. Chem. 193 (1951) 265–275.
[29] J. Murphy, J.P. Riley, A single-solution method for the determination of soluble phosphate in sea waters, J. Mar. Biol. Ass. U.K. 37 (1958) 9–14.
[30] A.E. Bennett, C.M. Rienstra, M. Auger, K.V. Lakshmi, R.G. Griffin, Heteronuclear decoupling in rotating solids, J. Chem. Phys. 103 (1995) 6951–6958.
[31] N. Bloembergen, On the interaction of nuclear spins in crystalline lattice, Physica 15 (1949) 386–426.
[32] D.M.J. Duer, Solid-state NMR spectroscopy principles and applications, Blackwell Science, 2002.
[33] B.M. Fung, A.K. Khitrin, K. Ermolaev, An improved broadband decoupling sequence for liquid crystals and solids, J. Magn. Reson. 142 (2000) 97–101.
[34] J. Czaplicki, G. Cornelissen, F. Halberg, GOSA, a simulated annealing-based program for global optimization of nonlinear problems, also reveals transyears, J. Appl. Biomed. 4 (2006) 87–94.
[35] T. Surrey, F. Jahnig, Refolding and oriented insertion of a membrane-protein into a lipid bilayer, Proc. Natl. Acad. Sci. U. S. A. 89 (1992) 7457–7461.
[36] N.K. Burgess, T.P. Dao, A.M. Stanley, K.G. Fleming, Beta-barrel proteins that reside in the *Escherichia coli* outer membrane in vivo demonstrate varied folding behavior in vitro, J. Biol. Chem. 283 (2008) 26748–26758.
[37] G.J. Patel, S. Behrens-Kneip, O. Holst, J.H. Kleinschmidt, The periplasmic chaperone skp facilitates targeting, insertion, and folding of OmpA into lipid membranes with a negative membrane surface potential, Biochemistry 48 (2009) 10235–10245.
[38] Z.V. Leonenko, E. Finot, H. Ma, T.E. Dahms, D.T. Cramb, Investigation of temperature-induced phase transitions in DOPC and DPPC phospholipid bilayers using temperature-controlled scanning force microscopy, Biophys. J. 86 (2004) 3783–3793.
[39] M. Hiller, L. Krabben, K.R. Vinothkumar, F. Castellani, B.-J. van Rossum, W. Kuhlbrandt, H. Oschkinat, Solid-state magic-angle spinning NMR of outer-membrane protein G from *Escherichia coli*, Chembiochem 6 (2005) 1679–1684.
[40] R. Koebnik, Structural and functional roles of the surface-exposed loops of the beta-barrel membrane protein OmpA from *Escherichia coli*, J. Bacteriol. 181 (1999) 3688–3694.
[41] Y. Wang, O. Jardetzky, Probability-based protein secondary structure identification using combined NMR chemical-shift data, Protein Sci. 11 (2002) 852–861.
[42] Y. Li, D.A. Berthold, R.B. Gennis, C.M. Rienstra, Chemical shift assignment of the transmembrane helices of DsbB, a 20-kDa integral membrane enzyme, by 3D magic-angle spinning NMR spectroscopy, Protein Sci. 17 (2008) 199–204.
[43] Y. Han, J. Ahn, J. Concel, I.-J.L. Byeon, A.M. Gronenborn, J. Yang, T. Polenova, Solid-state NMR studies of HIV-1 capsid protein assemblies, J. Am. Chem. Soc. 132 (2010) 1976–1987.
[44] A. McDermott, T. Polenova, A. Bockmann, K.W. Zilm, E.K. Paulsen, R.W. Martin, G.T. Montelione, Partial NMR assignments for uniformly (C-13, N-15)-enriched BPTI in the solid state, J. Biomol. NMR 16 (2000) 209–219.
[45] M. Etzkorn, S. Martell, O.C. Andronesi, K. Seidel, M. Engelhard, M. Baldus, Secondary structure, dynamics, and topology of a seven-helix receptor in native membranes, studied by solid-state NMR spectroscopy, Angew. Chem. 46 (2007) 459–462.
[46] R.A. Venters, B.T. Farmer, C.A. Fierke, L.D. Spicer, Characterizing the use of perdeuteration in NMR studies of large proteins C-13, N-15 and H-1 assignments of human carbonic anhydrase II, J. Mol. Biol. 264 (1996) 1101–1116.
[47] P.J. Spooner, R.H. Friesen, J. Knol, B. Poolman, A. Watts, Rotational mobility and orientational stability of a transport protein in lipid membranes, Biophys. J. 79 (2000) 756–766.
[48] A.G. Palmer, J. Williams, A. McDermott, Nuclear magnetic resonance studies of biopolymer dynamics, J. Phys. Chem. 100 (1996) 13293–13310.
[49] N. Giraud, M. Blackledge, M. Goldman, A. Bockmann, A. Lesage, F. Penin, L. Emsley, Quantitative analysis of backbone dynamics in a crystalline protein from nitrogen-15 spin–lattice relaxation, J. Am. Chem. Soc. 127 (2005) 18190–18201.
[50] J. Yang, M.L. Tasayco, T. Polenova, Dynamics of reassembled thioredoxin studied by magic angle spinning NMR: snapshots from different time scales, J. Am. Chem. Soc. 131 (2009) 13690–13702.
[51] V. Chevelkov, U. Fink, B. Reif, Quantitative analysis of backbone motion in proteins using MAS solid-state NMR spectroscopy, J. Biomol. NMR 45 (2009) 197–206.
[52] G. Reuther, K.T. Tan, A. Vogel, C. Nowak, K. Arnold, J. Kuhlmann, H. Waldmann, D. Huster, The lipidated membrane anchor of full length N-Ras protein shows an extensive dynamics as revealed by solid-state NMR spectroscopy, J. Am. Chem. Soc. 128 (2006) 13840–13846.
[53] J.R. Lewandowski, J. Sein, H.J. Sass, S. Grzesiek, M. Blackledge, L. Emsley, Measurement of site-specific ^{13}C spin–lattice relaxation in a crystalline protein, J. Am. Chem. Soc. 132 (2010) 8252–8254.
[54] J. Yang, L. Aslimovska, C. Glaubitz, Molecular dynamics of proteorhodopsin in lipid bilayers by solid-state NMR, J. Am. Chem. Soc. 133 (2011) 4874–4881.
[55] H. Nikaido, M. Vaara, Molecular-basis of bacterial outer-membrane permeability, Microbiol. Rev. 49 (1985) 1–32.
[56] H. Keweloh, G. Weyrauch, H.J. Rehm, Phenol-induced membrane-changes in free and immobilized *Escherichia-coli*, Appl. Microbiol. Biotechnol. 33 (1990) 66–71.
[57] H. Nikaido, Molecular basis of bacterial outer membrane permeability revisited, Microbiol. Mol. Biol. Rev. 67 (2003) 593–656.
[58] H. Heise, W. Hoyer, S. Becker, O.C. Andronesi, D. Riedel, M. Baldus, Molecular-level secondary structure, polymorphism, and dynamics of full-length alpha-synuclein fibrils studied by solid-state NMR, Proc. Natl. Acad. Sci. U. S. A. 102 (2005) 15871–15876.
[59] O.C. Andronesi, S. Becker, K. Seidel, H. Heise, H.S. Young, M. Baldus, Determination of membrane protein structure and dynamics by magic-angle-spinning solid-state NMR spectroscopy, J. Am. Chem. Soc. 127 (2005) 12965–12974.
[60] B. Liang, A. Arora, L.K. Tamm, Fast-time scale dynamics of outer membrane protein A by extended model-free analysis of NMR relaxation data, Biochim. Biophys. Acta - Biomembr. 1798 (2010) 68–76.
[61] P.M. Hwang, R.E. Bishop, L.E. Kay, The integral membrane enzyme PagP alternates between two dynamically distinct states, Proc. Natl. Acad. Sci. U. S. A. 101 (2004) 9618–9623.
[62] D. Datta, N. Vaidehi, W.B. Floriano, K.S. Kim, N.V. Prasadarao, W.A. Goddard III, Interaction of *E. coli* outer-membrane protein A with sugars on the receptors of the brain microvascular endothelial cells, Proteins 50 (2003) 213–221.
[63] N.V. Prasadarao, Identification of *Escherichia coli* outer membrane protein A receptor on human brain microvascular endothelial cells, Infect. Immun. 70 (2002) 4556–4563.
[64] M. Pichavant, Y. Delneste, P. Jeannin, C. Fourneau, A. Brichet, A.B. Tonnel, P. Gosset, Outer membrane protein a from *Klebsiella pneumoniae* activates bronchial epithelial cells: implication in neutrophil recruitment, J. Immunol. 171 (2003) 6697–6705.
[65] T.A. Pascal, R. Abrol, R. Mittal, Y. Wang, N.V. Prasadarao, W.A. Goddard, Experimental validation of the predicted binding site of *Escherichia coli* K1 outer membrane protein A to human brain microvascular endothelial cells: identifications of critical mutations that prevent *E. Coli* meningitis, J. Biol. Chem. 285 (2010) 37753–37761.
[66] N.V. Prasadarao, R. Mittal, S. Krishnan, I. Gonzalez-Gomez, Deciphering the roles of outer membrane protein A extracellular loops in the pathogenesis of *Escherichia coli* K1 meningitis, J. Biol. Chem. 286 (2011) 2183–2193.

Supplementary Information

Dynamics of *Klebsiella pneumoniae* OmpA transmembrane domain: the four extracellular loops display restricted motion behavior, in micelles and in lipid bilayers.

Iordan Iordanov[a,b], Marie Renault[c], Valérie Réat[a,b], Patrick D. Bosshart[d], Andreas Engel[e], Olivier Saurel[a,b], Alain Milon[a,b *]

[a)] Institute of Pharmacology and Structural Biology, Université de Toulouse – UPS, 205 route de Narbonne, 31077, Toulouse, France

[b)] IPBS – UMR 5089, CNRS, 205 route de Narbonne, BP 64182, 31077 Toulouse, France

[c)] UPCAM iSm2 service 512, Campus Scientifique de St Jérôme, 13397 Marseille cedex 20

[d)] Department of Biosystems Science and Engineering, ETH Zurich, CH-4058 Basel, Switzerland

[e)] Department of Pharmacology, Case Western Reserve University, Cleveland, OH 44106, USA

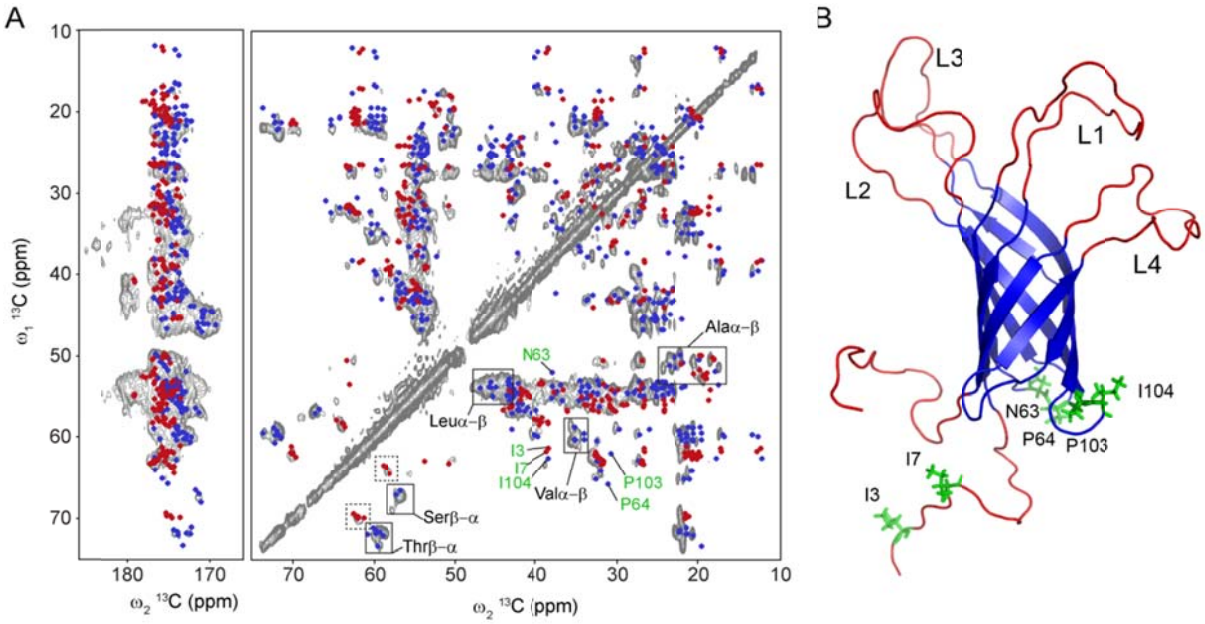

Supplementary Fig. 1. (A) Two-dimensional ^{13}C-^{13}C PDSD correlation spectrum of the membrane-embedded KpOmpA TM domain reconstituted in *E. coli* PLE vesicles (PLR=0.5, w/w) recorded with a PDSD mixing time of 40 ms at a MAS frequency of 12 kHz and at 20°C (sample temperature). Expected intraresidue C-C correlations predicted from solution NMR chemical shifts of KpOmpA TM domain (BMRB accession code: 15651) after correction for isotope effect (squares). **(B)** Cartoon representation of the solution NMR structure of KpOmpA TM domain (PDB accession code: 2K0L). Color-coding in (A) and (B): red, extracellular loops (L1 to L4), N- and C-term extremities; blue, transmembrane β-sheets (β1 to β8) and periplasmic turns (T1 to T3). Residues with backbone C^{α}/C^{β} correlations that could not be observed at similar peak position than those predicted by solution NMR chemical shifts are labeled in green.


Protein
Extracellular loop
L1
□□□□ooooooo●●●●●●*●●●●●●
K.pneumoniae OmpA SQYHDTGFYGNGFQNNNGPTRNDQ
E.coli ompA1 QYHDTGFI-----NNNGPTHENQ
E.coli ompA2 QYHDTGFI-----PNNGPTHENQ
L2
□□□ooooooooooo□oo
K.pneumoniae OmpA LGRMAYKGSVDNGAFKA
E.coli ompA1 LGRMPYKGSVENGAYKA
E.coli ompA2 LGRMPYKGDNINGAYKA
L3
oooooo●●●●●●●●●●
K.pneumoniae OmpA DSKGNYASTGVSRSEH
E.coli ompA1 ADTKSNVYG-----KNH
E.coli ompA2 ADTKANVPG-GASFKDH
L4
□□□□□□□□ooooooooo□□□o
K.pneumoniae OmpA QWVNNIGDAGTVGTRPDNGM
E.coli ompA1 WTNNIGDAHTIGTRPDNGM
E.coli ompA2 WTNNIGDAHTIGTRPDNGM

Supplementary Fig. 2. Alignment of the loop regions of OmpA proteins from *K.pneumoniae* and the two OmpA alleles found in *E.coli*. "*K.pneumoniae* OmpA" denotes the sequence of KpOmpA used in this study. This sequence is derived from *K.pneumoniae* strain Rv 308 and exhibits 100% sequence identity with KpOmpA from *K.pneumoniae* subsp. *rhinoscleromatis* (ATCC 13884), causing rhinoscleroma (a respiratory tract infection). The loop segments are according to the solution state NMR structure of KpOmpA (PDB ID: 2K0L, [1]). "*E.coli ompA1*" denotes the "classic" OmpA sequence from the "domesticated" *E.coli* K-12 laboratory strain. The loop segments of *ompA1* are according to the solution state NMR structure of OmpA (PDB ID: 2GE4, [2]), which was acquired on artificially expressed transmembrane domain of OmpA with identical to the *E.coli* K-12 loop regions. "*E.coli ompA2*" denotes the OmpA sequence from the *E.coli* strain ABU 83972, responsible for bacteriuria. The four loop frames in *ompA2* are considered the same as in *ompA1*. The variable amino acids on each chain are indicated with white letters on a black background. For clarity and to emphasize the more significant variations within the amino acid compositions, the homologous pairs of I-V, F-Y and D-E are not indicated. For the KpOmpA sequence only, unassigned residues experiencing restricted mobility due to conformational exchange processes (in the ms-μs timescale) are indicated with open squares (□); assigned residues with random coil chemical shifts that still exhibit restricted mobility are denoted with open circles (○); finally, the most mobile residues (with isotropic motions in the ps/ns to μstimescale) are indicated with filled circles (●). The asterisk (*) denotes a single residue (G45) that belongs to the highly dynamic region of L1 but remained unassigned. Note that the variable dynamic behavior of the different regions correlates with their levels of evolutional preservation.

[1] M. Renault, O. Saurel, J. Czaplicki, P. Demange, V. Gervais, F. Lohr, V. Reat, M. Piotto, A. Milon, Solution state NMR structure and dynamics of KpOmpA, a 210 residue transmembrane domain possessing a high potential for immunological applications, J. Mol. Biol., 385 (2009) 117-130.
[2] A. Arora, F. Abildgaard, J.H. Bushweller, L.K. Tamm, Structure of outer membrane protein A transmembrane domain by NMR spectroscopy, Nat. Struct. Biol., 8 (2001) 334-338.